EarlyView publication on wileyonlinelibrary.com
(issue and page numbers not yet assigned;
citable using Digital Object Identifier – DOI)

Phys. Status Solidi B, 1–9 (2012) / DOI 10.1002/pssb.201100002

physica status solidi b
www.pss-b.com
basic solid state physics

Possible existence of field-induced Josephson junctions

Krzysztof Pomorski*,[1,2] and Przemyslaw Prokopow[3]

[1] Institute of Theoretical Physics, Faculty of Physics, University of Warsaw, Poland
[2] Department of Physics, Institute of Physics, Astronomy and Computer Science, Jagiellonian University, Poland
[3] RIKEN, Institute of Physical and Chemical Research, Japan

Received 18 November 2011, revised 20 May 2012, accepted 8 June 2012
Published online 10 July 2012

Keywords extended Ginzburg–Landau formalism, field-induced Josephson junctions, nonlinear Josephson junctions, relaxation methods, superconducting ferromagnets

* Corresponding author: e-mail kdvpomorski@gmail.com, Phone: +48-728-384-555, Fax: (48) 22 6219475

We demonstrate the possible existence of a new class of superconducting Josephson junctions (JJs) named field-induced Josephson junctions (FIJJs). One representative is a junction made by placing a ferromagnetic strip on the top of a superconducting strip, which we study in this work. We obtain a possible transition between one regime of an FIJJ, which is the quasi-tunneling weak link Josephson junction (similar in certain aspects to an S–F–S Josephson junction, but with different boundary conditions), and the second regime of an FIJJ, which is the weak link constriction (two superconductors connected by a narrow superconducting link) as a function of the thickness of the superconducting strip, magnitude of magnetization, and temperature. We use the generalized Ginzburg–Landau (GL) equations derived from the extended Hubbard model in order to determine some properties of the new class of Josephson junction. In this paper, we perform the computation for a first type of superconductor, although both types of superconductor can be used to create an FIJJ. Further directions of studies of the indicated class of Josephson junction are also described.

1 Motivation Currently, large-scale complementary metal–oxide–semiconductor (CMOS) integrated circuits are used on a massive scale for electromagnetic (EM) signal processing with GHz frequencies. Most electronics is implemented with this technology. However, there are serious limitations in increasing the speed of semiconductor circuit operation with the growth of the semiconductor circuit integration scale. The main obstacle is the power dissipation in such circuits. One way to achieve the increase in both parameters of integrated circuits is the use of high-integration superconducting circuits, which can operate almost without dissipation with very high frequencies as in the THz range. Such superconducting circuits should be based on Josephson junctions, which can operate in the THz range and which can be manufactured in a relatively easy way. Another requirement for low operation cost and massive use is the need for Josephson junction circuit operation at higher temperatures. This can be satisfied by usage of high-temperature superconductors that can superconduct at the temperature of liquid nitrogen. Additional motivation for the studies of Josephson junctions (first described as tunneling junctions by Josephson [1] and later developed also as weak links by many physicists, *e.g.*, by Likharev [2]) is a possible implementation of qubits in high-temperature superconductors that can be easily implemented on a massive scale. A very promising superconducting candidate for high-temperature applications in THz circuit design and possible high temperature superconducting qubit implementation is the field-induced Josephson junction (FIJJ), made by placing a ferromagnetic strip on the top of an *s*- or *d*-wave superconducting strip (or possibly any other superconductor type). In order to understand the physics of FIJJs and their architectures, we use the relaxation method to solve equations obtained by the extended Ginzburg–Landau (GL) formalism and within the Bogoliubov–de Gennes (BdGe) formalism. Solutions of GL and BdGe equations for the case of FIJJs give the basis for the determination of transport properties of a new class of Josephson junctions that is described in the next sections.

2 Definition of field-induced Josephson junction We consider a class of the FIJJ in the first type of superconductor. One of the first works in this direction was started by Clinton [3]. Such a Josephson junction was made by placing a non-superconducting element, *e.g.*, a ferromagnet (MFIJJ – magnetic FIJJ) or a multiferroic one on the top of a superconducting strip (EFIJJ – electric FIJJ or MEFIJJ – magneto-electric FIJJ), as described in Fig. 1 with its circuit representation. In all types of FIJJ a modulation of the superconducting order parameter is achieved in the superconductor due to the presence of the non-superconducting strip on the top of the superconductor, which leads to the creation of two or more superconducting reservoirs. Partial reservoir overlap and the Cooper pair tunneling between them (as pointed out in Refs. [1] and [2]) leads to the Josephson effect. Some experiments with such a class of Josephson junctions were conducted in Refs. [4, 5] and [6] with a MFIJJ [11]. The modulation of the superconducting order parameter (SCOP) is due to the existence of the magnetic, electric, or combined electric and magnetic field coming from the non-superconducting element. It is also due to the diffusion of Cooper pairs from the superconductor to the non-superconducting element and due to diffusion of unpaired electrons from the non-superconducting element to the superconductor, as described in Ref. [7]. Those effects are accounted for by the GL or BdGe formalism and are the subject of the computations conducted in this work. Since modulation of the order parameter is due to the existence of an electric or magnetic field, we call such a Josephson junction an EFIJJ, an MFIJJ, or an electric (magnetic) FIJJ. In general, we refer to such a class of Josephson junction as the FIJJ. If we replace the ferromagnetic element of an FIJJ by non-ferromagnetic and non-superconducting elements, we obtain a system that can show a different Josephson junction behavior. We call such a structure an unconventional Josephson junction (uJJ). It is also interesting to find an analogy between the FIJJ and the field-effect transistor (FET). In both cases the electric (or magnetic) field can be used to make a transistor where the flow of an external electric current via the device is induced by the presence of the electric field. In the case of an FET, the presence of the electric field is due to the voltage applied to the gate, which is placed between drain and source. If we use a multiferroic material on the top of the superconductor and apply a certain voltage between "source" and "drain", we induce a certain magnetic field. Thus, we obtain the modulation of the superconducting order parameter by means of the electric and magnetic field. The influence of the electric field on tuning properties of the superconductor is described in Ref. [10].

In this work we show the behavior regimes of the MFIJJ and its circuit representation as depicted in Fig. 1. We expect that the junction(s) circuit parameters C, L, R (capacitance, inductance, resistance) can be tuned by the magnetization $\boldsymbol{M}$ of the ferromagnetic bar, the external magnetic field $\boldsymbol{B}$, and the electric current I flowing via the system.

3 Mathematical description of FIJJ There are various formalisms describing superconductors, from phenomenological and simple to fundamental and complex ones such as: two-fluid model, GL, BdGe [20], Usadel [15], Eilenberger [16], Gorkov and Keldysh formalisms. The complexity in solving equations in the given formalisms increases as we move from the most phenomenological toward a more microscopic picture. The good example is a comparison of Ginzburg-Landau and Gorkov formalism as given by [17]. In this work we describe only the MFIJJ system. The superconductor–ferromagnet system was studied by many groups with use of various formalisms, as is indicated in Ref. [23]. To begin, we use the GL formalism, which gives the information about the SCOP distribution for

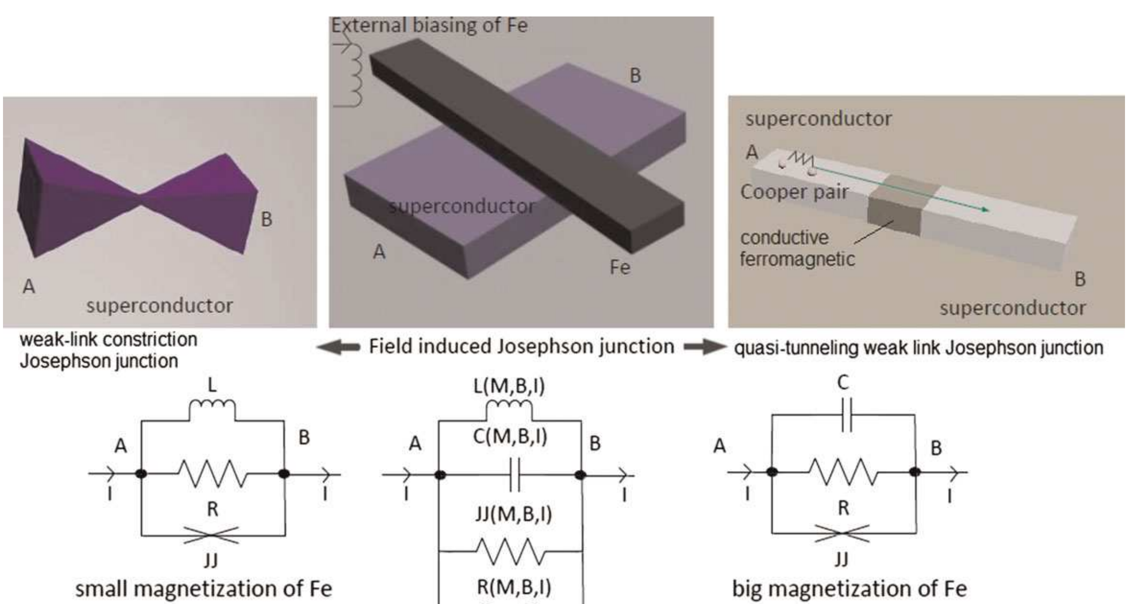

Figure 1 (online color at: www.pss-b.com) Behavior regimes of MFIJJ and its circuit representation.

temperatures close to the critical temperature T_c. We will consider only occurrence of the first kind of superconductor, which transits to the normal state under the influence of a magnetic field. GL theory of an s-wave superconductor with a ferromagnetic strip on the top gives the free energy functional F that is the sum of the following terms: superconductor term F_s, ferromagnetic bar term F_M and term describing superconductor–ferromagnet interaction $F_{s\text{–}M}$. Thus, we obtain $F = F_s + F_M + F_{s-M}$, where

$$F_M = \int \mathrm{d}^3 r \left(a(T)|\boldsymbol{M}|^2 + \frac{b(T)}{2}|\boldsymbol{M}|^4 + C|\nabla \boldsymbol{M}|^2 \right), \qquad (1)$$

$$F_s = \int \mathrm{d}^3 r \left(\frac{\alpha}{2}|\psi|^2 + \frac{\beta}{4}|\psi|^4 + \frac{1}{2m}\left| \left(\frac{\hbar}{i}\nabla - \frac{2e}{c}\boldsymbol{A} \right)\psi \right|^2 + \frac{(\mathrm{curl}\boldsymbol{A})^2}{4\pi} \right), \qquad (2)$$

$$F_{s,M} = \int \mathrm{d}^3 r \left(\gamma|\psi|^2|\boldsymbol{M}|^2 + \varepsilon|\nabla \boldsymbol{M}|^2|\psi|^2 + \frac{\mu}{2m}\left| \left(\frac{\hbar}{i}\nabla - \frac{2e}{c}\boldsymbol{A} \right)\psi \right|^2 |\boldsymbol{M}|^2 + \mathrm{curl}(\boldsymbol{A})\boldsymbol{M} \right). \qquad (3)$$

By ψ we denote the complex scalar field describing the SCOP while the vector fields $\boldsymbol{A}$ and $\boldsymbol{M}$ describe the vector potential and the magnetization. In the case of the superconductor–ferromagnet system, by minimizing the functional $F = F_s + F_M + F_{s,M}$ and applying $\delta F/\delta\psi = 0$ we obtain

$$\left(\alpha + \gamma|\boldsymbol{M}|^2 \right)\psi + \beta|\psi|^2\psi - \frac{\hbar^2}{2m}\left(1 + \mu|\boldsymbol{M}|^2 \right)\nabla^2\psi = 0,$$

and by $\delta F/\delta A = 0$ we get the equation for the electric current density

$$\boldsymbol{j} = \frac{e}{\hbar i m}\left(1 + \mu|\boldsymbol{M}|^2 \right)\left(\psi^\dagger\nabla\psi - \psi\nabla\psi^\dagger \right) - \frac{e^2\boldsymbol{A}}{2mc}\left(1 + \mu|\boldsymbol{M}|^2 \right)\psi.$$

The boundary condition between the s-wave superconductor and normal metal is given as

$$\underline{n}\Pi\psi(x) = \underline{n}\left(\frac{\hbar}{i}\nabla - \frac{2e}{c}\boldsymbol{A}(x) \right)\psi(x) = \frac{1}{b}\psi(x),$$

where $\underline{n}$ is the unit vector perpendicular to the superconductor–other medium (as normal metal) interface, b is the constant depending on the material as $b = (N_s D_s / N_n D_n)\xi$, where N_s and N_n are the densities of states at the Fermi level in a superconductor and in a normal metal at the Fermi level, ξ is the superconducting coherence length, and D_s and D_f are diffusion constants correlated to the Fermi velocity and relaxation time. The constant b can be expressed by means of the Usadel formalism [9, 11].

A quite similar mathematical structure can be assigned to the description of an EFIJJ. In such a case the GL equations have to describe a multiferroic–superconductor system. The boundary conditions for this case are given in Ref. [11]. We obtain the following equations:

$$F_E = \int \mathrm{d}^3 r \left(a_1(T)|\boldsymbol{P}|^2 + \frac{b_1(T)}{2}|\boldsymbol{P}|^4 + C_1|\nabla \boldsymbol{P}|^2 \right), \qquad (4)$$

$$F_s = \int \mathrm{d}^3 r \left(\alpha|\psi|^2 + \beta|\psi|^4 + \frac{1}{2m}\left| \left(\frac{\hbar}{i}\nabla - \frac{2e}{c}\boldsymbol{A} \right)\psi \right|^2 + \frac{(\mathrm{curl}\boldsymbol{A})^2}{4\pi} \right), \qquad (5)$$

$$F_{s,P} = \int \mathrm{d}^3 r \left(\gamma_1|\psi|^2|\boldsymbol{P}|^2 + \frac{\mu}{2m}\left| \left(\frac{\hbar}{i}\nabla - \frac{2e}{c}\boldsymbol{A} \right)\psi \right|^2 \times |\boldsymbol{P}|^2 + \varepsilon_1|\nabla \boldsymbol{P}|^2|\psi|^2 \right), \qquad (6)$$

where $F = F_s + F_E + F_{s,E}$. Therefore, the three-dimensional magnetization field $\boldsymbol{M} = (M_x, M_y, M_z)$ is replaced with the three-dimensional electric polarization field $\boldsymbol{P} = (P_x, P_y, P_z)$. Having the order parameter distributions from the solution of GL equations as in the case of a non-superconducting and non-ferromagnetic element on the top of a superconductor, we place them into the BdGe equations and obtain eigenvalues and eigenfunctions, which determine the local density of states (LDOS) given by the formula

$$N(r,E) = -\sum_n \left(f'(\varepsilon_n - E)|u_n(r)|^2 + f'(\varepsilon_n + E)|v_n(r)|^2 \right) \qquad (7)$$

(see Ref. [20]), where f is the Fermi–Dirac distribution function (u_n, v_n) and ε_n are eigenfunctions and eigenvalues of the BdGe equation and the summation is performed over the energies below the Debye frequency. Initially, the GL equation was solved for the case of zero magnetic field for the two-dimensional case. Once the SCOP is determined from the GL equation, we substitute it into the BdGe equations. In such a way the LDOS was obtained inside the superconductor for the structure with a non-superconductor placed on the top of a superconductor, as indicated in Fig. 2, and when the vector potential and magnetization are set to zero.

4 Computation method There are various methods which can be used to solve the GL equations such as the finite-difference method, spectral methods, annealing

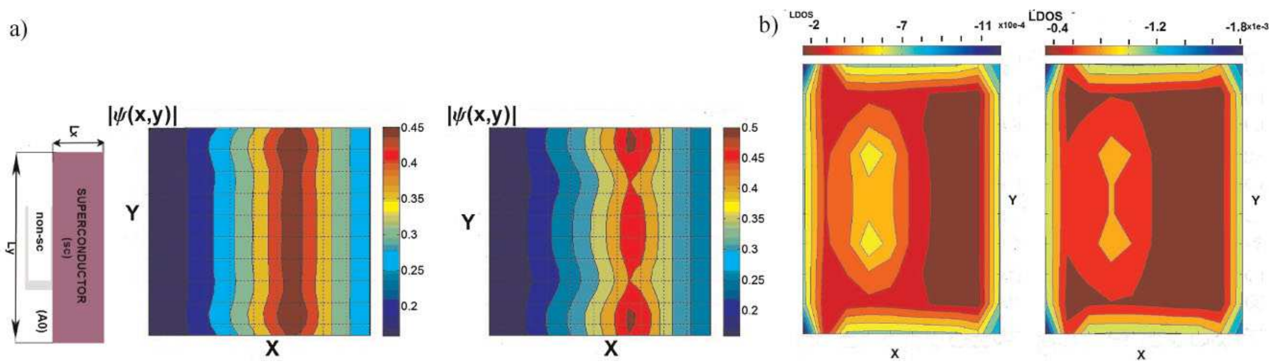

Figure 2 (online color at: www.pss-b.com) SCOP distribution and the LDOS in s-wave uJJ with no magnetic field. (a) Geometry and s-wave SCOP distribution $\psi(x, y)$ for a normal strip on the top of a superconducting strip with no magnetic field (case of uJJ). Decrease in thickness of the superconducting strip (from left to right) has its impact on the separation of Cooper pair reservoir into two reservoirs. (b) LDOS for two-dimensional s-wave uJJ Josephson junction (FIJJ architecture with no magnetic field) for different temperatures T_1 and T_2, where $T_1 < T_2$.

methods, and many others. Because of simplicity and numerical stability even for the case of a complex set of nonlinear equations, the relaxation method is used. Deriving the GL equations we look for the case of the functional derivative of the free energy functional F set to zero with respect to the physical fields upon which it depends. Then we obtain the following class of equations:

$$\frac{\delta}{\delta X_i} F[\psi, \boldsymbol{A}, \boldsymbol{M}, \boldsymbol{E}] = 0, \quad X_i = (\psi, \boldsymbol{A}, \boldsymbol{M}, \boldsymbol{E}), \tag{8}$$

where $\boldsymbol{E}$ is the electric field.

To approach the solutions given as the configuration of the (ψ, $\boldsymbol{M}$, $\boldsymbol{A}$, $\boldsymbol{E}$) fields we need to make the initial guess of physical fields configuration and of the SCOP in the given space, using physical intuition. The initial guess should be not too far from the solution. Having the initial guess, we perform the calculation of the fields change on the given lattice, with each iteration virtual time step δt according to the scheme

$$\frac{\delta}{\delta X_i} F[\psi, \boldsymbol{A}, \boldsymbol{M}, \boldsymbol{E}] = -\eta_i \frac{\delta X_i}{\delta t}, \quad X_i = (\psi, \boldsymbol{A}, \boldsymbol{M}, \boldsymbol{E}). \tag{9}$$

Here, η_1, η_2, η_3, η_4 are phenomenological constants. The δt term cannot assume too big a value since it might bring a numerical instability in the simulation. One of the signatures of approaching the solution is the minimization of the free energy functional. In this case one can observe a characteristic plateau in the free energy as a function of iteration (virtual time). It should be emphasized that the relaxation method applied here is in the framework of the GL formalism and it can also be conducted with the use of the Greens function technique in the Usadel or Eilenberger form.

5 Computation results The first computations we conducted for the case of a non-superconducting strip being placed on the top of a superconducting strip in two and three dimensions with no magnetization or vector potential present in the system. Because of the presence of the non-superconducting strip, there occurs a diffusion of Cooper pairs from the superconductor to the normal strip, as well as a diffusion of unpaired electrons from the non-superconducting strip into the superconductor, which is effectively visible as a lowering of the SCOP inside the superconducting strip.

Depending on the thickness of the superconducting strip we have identified two different regimes of the GL solution. The first regime is obtained when the superconducting strip is thick in comparison with the non-superconducting strip. Then, lowering of the SCOP inside the superconductor does not lead to the separation of the superconducting region into two regions, as indicated by the middle plot of Fig. 2a.

The second regime occurs when the superconducting strip is very thin, which is indicated in the right picture of Fig. 2a. The lowering of concentration of Cooper pairs in the middle of the superconducting strip brings an effective separation of the superconducting reservoir into two parts. In such a case we expect the occurrence of the Josephson effect in this structure by the interaction of two overlapping superconducting reservoirs.

We can intuitively state that weak separation of Cooper pair reservoirs by a geometrical factor tunes the Josephson effect occurring in the structure. The geometrical configuration of the studied structure is depicted by the left picture of Fig. 2a.

In the performed computations the used dimensions of the structure are $(L_x, L_y, L_z) = (0.6, 20, 20)$ and (0.2, 20, 20) in the superconducting coherence length units.

Another possibility is the separation of the superconducting reservoir into two or more reservoirs by means of a magnetic field, which gives the basis for the possible existence of the induced Josephson effect in such systems. By changing the magnetization strength of the ferromagnetic bar (as *e.g.*, Fe) we can tune the Josephson junction properties from the constriction weak link to the quasi-tunneling weak link regime. The distribution of magnitude of the SCOP and of the magnetization inside the superconductor for various magnetizations of the Fe bar is depicted

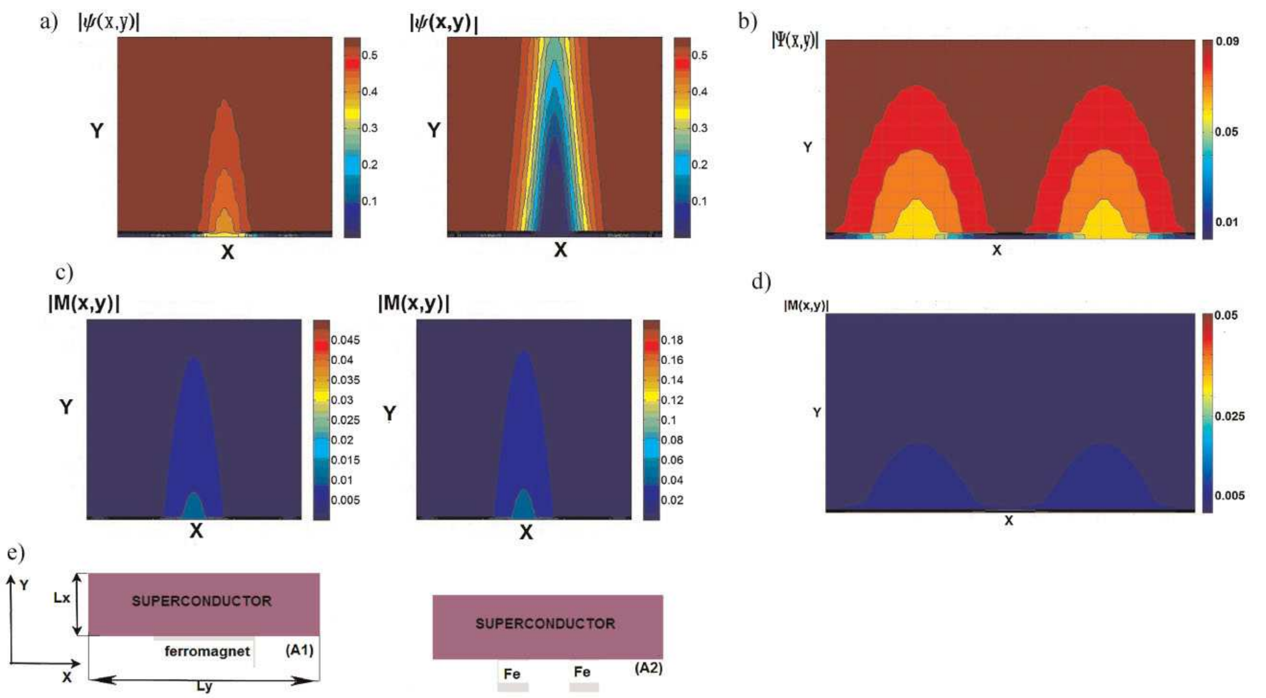

Figure 3 (online color at: www.pss-b.com) Characterization of s-wave FIJJ Josephson junction(s) tuning properties. (a) Two-dimensional SCOP distribution $|\psi(x,y)|$ in magnetic field FIJJ for different magnetizations of the ferromagnetic bar (A1 configuration). The transition from the quasi-tunneling weak link Josephson junction to the weak link constriction can be observed. (b) Two-dimensional SCOP distribution $|\psi(x,y)|$ in two-MFIJJ array (A2 configuration). (c) Two-dimensional magnetization distribution inside superconductor $|M(x,y)|$ in FIJJ for different magnetizations of the ferromagnetic bar (A1). The higher the magnetization, the more effective the division of the SCOP reservoir is observed (as we move from left to right). Therefore, the transition from the constriction weak link to the quasi-tunneling weak link Josephson junction occurs. (d) Two-dimensional magnetization distribution $|M|$ inside superconductor of two-MFIJJ asymmetric array (A2), where $|M|=\sqrt{M_x^2+M_y^2}$. (e) Different geometries of FIJJ(s) (A1 and A2 configurations).

in Figs. 3 and 4 by the numerical solution of Eqs. (1), (2), and (3), with use of the relaxation method. In Fig. 3 the two-dimensional superconducting order parameter distribution $\psi(x,y)$ in a magnetic field FIJJ for two different magnetizations of the ferromagnetic bar is depicted. The dimensional lattice of size 70×70 was used for the computations. The geometrical configuration of the superconductor–ferromagnet system is denoted as A1 (ferromagnetic strip under superconductor strip) and is depicted in Fig. 3e (left). The size of the studied structure in terms of superconducting coherence length units is given by two parameters $(L_x, L_y)=(1.4, 42.2)$. The transition from the quasi-tunneling weak link Josephson junction to the weak link Josephson junction constriction can be observed. The quasi-tunneling weak link is named after the structure that has the continuous superconductor material, but the magnetic field lowers locally the SCOP and it introduces locally a non-zero magnetization in the area where the superconductivity order is destroyed. In such a case the system has similarity to the case of the tunneling S–F–S Josephson junction. In both FIJJ regimes the magnetization is increased locally and the SCOP is destroyed locally. There is however a key difference. In S–F–S material there is the interface discontinuity and usually the boundary condition

$$\underline{n}\Pi\psi(x)=\underline{n}\left(\frac{\hbar}{i}\nabla-\frac{2e}{c}\boldsymbol{A}(x)\right)\psi(x)=\frac{1}{b}\psi(x)$$

takes place. Such a situation does not occur in an FIJJ quasi-tunneling weak link in the direction of the current flow. If the magnetization of the FIJJ is weak, then there is no strong penetration of the magnetic field inside the superconductor area. Nevertheless, the lowering of the SCOP is visible, so the system is similar to the weak link constriction. In the conducted simulations the magnetization of the Fe strip was assumed to be constant inside Fe. By the continuous change of the magnetic strip magnetization, the continuous change of the SCOP strength and of the magnetization inside the superconductor has been achieved. Thus, we claim to observe the transition between the quasi-tunneling weak link FIJJ and the FIJJ weak link constriction. The same simulation was repeated for the case of more than one FIJJ.

In Fig. 4 the distribution of the s-wave SCOP $|\psi(x,y)|$ and the magnetization $M(x,y)|$ inside the superconductor for a two asymmetric FIJJ array with magnetized Fe elements in the direction perpendicular to the S–F interface is depicted.

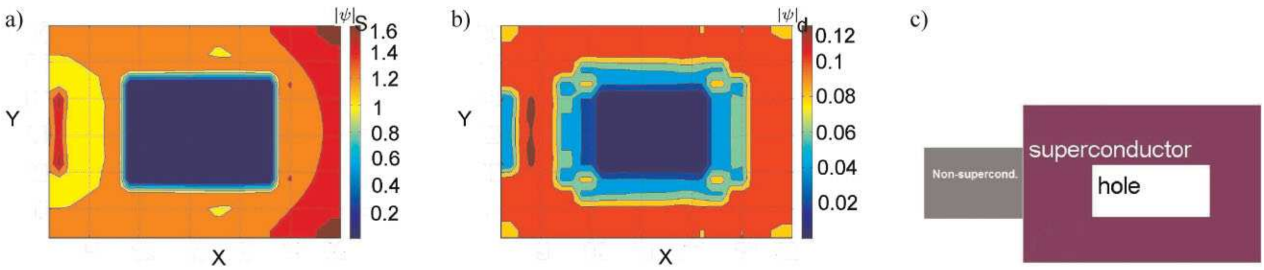

Figure 4 (online color at: www.pss-b.com) SQUID made of uJJ for *d*-wave superconductors with no magnetic field. (a) *s*-wave SCOP distribution in *d*-wave uJJ SQUID. (b) *d*-wave SCOP distribution in *d*-wave uJJ SQUID. (c) Topology of *d*-wave uJJ SQUID. *c*-axis is perpendicular to the picture plane.

The structure is in the configuration A2 (2FIJJs on the same side of the superconductor, as given on the right-hand side of Fig. 3e) with dimensions $(L_x, L_y) = (0.7, 21)$ in the superconducting coherence length units. In all conducted computations the demagnetization effects were taken into account by means of the GL formalism and they do not affect significantly the obtained distribution of the SCOP close to the F strip.

It is possible to determine the SCOP distribution in an EFIJJ in a similar way as in the case of an MFIJJ, when a multiferroic element is used instead of the ferromagnet.

This is because the mathematical structure of the system free energy functional is quite analogous to the GL free energy used for the MFIJJ case, as indicated in Eqs. (1)–(3) and (4)–(6). In such a case, it seems to be very desirable to extend the GL formalism further to account for the existence of non-zero magnetization and non-zero electric field.

In the future we plan to solve the extended GL equations for the case of *d*-wave superconductors and to account for the coexistence of singlet and triplet phases. The presence of *s*-wave or *d*-wave SCOP components will be possible in the extended GL framework, which is equivalent to the coexistence of five coupled complex scalar fields (p_x, p_y, p_z, s, d) in three-dimensional or two-dimensional cases. The detailed coefficients of the GL functional can be obtained from the paper by Kuboki [13]. It is also interesting to analyze the non-uniform BdGe wavepacket reflections and, in particular, the Andreev reflection in the studied structure for *s*-wave and *d*-wave superconductors.

Using our generalized methodology of the relaxation method that was presented in Ref. [8], we study now properties of an unconventional SQUID. It is made by placing a non-superconducting element close to the ring shape or rectangular shape superconductor, which reduces the SCOP in its neighborhood and thus creates possibly a weak link. The possible geometry of such a structure is depicted in Fig. 4c for the *d*-wave superconductor in the absence of magnetic or electric fields. Note that the proximity of a defect such as the occurrence of a non-superconducting strip in contact with a *d*-wave superconductor strip lowers the magnitude of the *d*-wave component of the order parameter and increases the magnitude of the *s*-wave component, as indicated in Fig. 4a and b. This is somehow similar to the situation around a vortex core induced by the external magnetic field in a *d*-wave superconductor [12]. Therefore, the given structure of FIJJ geometry of a *d*-wave superconductor with no magnetization and no magnetic field should not always be recognized as a weak link Josephson junction. A further study of this structure in the case of non-zero magnetic field is needed. We denote our uJJ as the structure with FIJJ geometry, but with no magnetization present as in the case of a normal strip on the top of a superconducting strip. Extending the GL $x^2 - y^2$ formalism to account for properties of a *d*-wave FIJJ in a wide temperature range is rather technical but it can be obtained from the microscopic model, as indicated in the work of Feder [21].

6 Coexistence of singlet and triplet phases in FIJJ

To account for the existence of singlet and triplet components, the extension of results of Ref. [2] from one to two dimensions is necessary.

Then in the general case of a *d*-wave superconductor–ferromagnet system the SCOP has five components $(\psi_s(x,y),\ \psi_d(x,y),\ \psi_{px}(x,y),\ \psi_{py}(x,y),\ \psi_{pz}(x,y))$ and three additional magnetization components occur as $(M_x(x,y),\ M_y(x,y),\ M_z(x,y))$, while the superconducting gap $\Delta(x,y)$ is given as

$$\Delta = \psi_s + \cos(2\phi)\psi_d + \cos(\phi_1)\psi_{px} + \cos(\phi_2)\psi_{py} + \cos(\phi_3)\psi_{pz}, \tag{10}$$

where ϕ depends on the crystal orientation and structure and ϕ_1, ϕ_2, ϕ_3 depend on the orientation and magnetization of the ferromagnetic bar and on the quality of the superconductor–ferromagnet interface.

In the conducted computations we have neglected the occurrence of the triplet component in the superconductor and the interaction term in the GL functional between superconducting triplet and singlet components, triplet superconductor order component and ferromagnet and also the term accounting for mutual interaction between singlet and triplet SCOPs and ferromagnet order parameter. Following Kuboki's derivation of the extended GL equations from the microscopical model [13, 14], we obtain a similar structure of free energy functional in the form

$$F = F_s + F_t + F_{st} + F_m + F_{sm} + F_{tm} + F_{stm} + F_{\mathrm{surf}}. \tag{11}$$

Denoting unit vectors in x and y directions by e_x and e_y and introducing the notation

$$D_{x(y)} = \frac{\hbar}{i}\partial_{x(y)} - \frac{2e}{c}A_{x(y)}, \tag{12}$$

$$D = e_x D_x + e_y D_y, \tag{13}$$

we obtain the following components of the free energy functional F:

$$\begin{aligned} F_s = \int \mathrm{d}^2 r \Big(& \alpha_s|\psi_s|^2 + \beta_s|\psi_s|^4 + K_s|\boldsymbol{D}\psi_s|^2 \\ & + \alpha_d|\psi_d|^2 + \beta_d|\psi_d|^4 + K_d|\boldsymbol{D}\psi_d|^2 + \gamma_1|\psi_s|^2|\psi_d|^2 \\ & + \gamma_1|\psi_s|^2|\psi_d|^2 + \gamma_2\big(\psi_d^2(\psi_d^*)^2 + c.c.\big) \\ & + K_{ds}\big((D_x\psi_d)(D_x\psi_s)^* - (D_y\psi_d)(D_y\psi_s)^* + c.c.\big)\Big), \end{aligned} \tag{14}$$

$$\begin{aligned} F_t = \int \mathrm{d}^2 r \Big(& \alpha_p(|\psi_{px}|^2 + |\psi_{py}|^2) + \beta_p(|\psi_{px}|^4 + |\psi_{py}|^4) \\ & + \gamma_{p1}|\psi_{px}|^2|\psi_{py}|^2 + \gamma_{p2}\big(\psi_{px}^2(\psi_{py}^*)^2 + c.c.\big) \\ & + K_{p1}(|D_x\psi_{px}|^2 + |D_y\psi_{py}|^2) \\ & + K_{p2}(|D_y\psi_{px}|^2 + |D_x\psi_{py}|^2) \\ & + K_{p3}\big((D_x\psi_{px})^*(D_y\psi_{py}) + c.c.\big) \\ & + K_{p4}\big((D_y\psi_{px})^*(D_x\psi_{py}) + c.c.\big)\Big), \end{aligned} \tag{15}$$

$$\begin{aligned} F_{st} = \int \mathrm{d}^2 r \Big(& \gamma_3(|\psi_{px}|^2 + |\psi_{py}|^2)|\psi_s|^2 \\ & + \gamma_4(|\psi_{px}|^2 + |\psi_{py}|^2)|\psi_d|^2 \\ & + \gamma_5\big((\psi_{px}^2 + \psi_{py}^2)(\psi_s^*)^2 + c.c.\big) \\ & + \gamma_6\big((\psi_{px}^2 + \psi_{py}^2)(\psi_d^*)^2 + c.c.\big) \\ & + \gamma_7(|\psi_{px}|^2 - |\psi_{py}|^2)(\psi_s^*\psi_d + c.c.) \\ & + \gamma_8(\psi_{px}^2 - \psi_{py}^2)(\psi_s^*\psi_d^* + c.c.)\Big), \end{aligned} \tag{16}$$

$$F_m = \int \mathrm{d}^2 r \Big(\alpha_m|\boldsymbol{M}|^2 + \beta_m|\boldsymbol{M}|^4 + K_m|\nabla\boldsymbol{M}|^2\Big), \tag{17}$$

$$F_{sm} = \int \mathrm{d}^2 r \Big(\gamma_{\mathrm{ms}}|\boldsymbol{M}|^2|\psi_s|^2 + \gamma_{\mathrm{md}}|\boldsymbol{M}|^2|\psi_{\mathrm{md}}|^2\Big), \tag{18}$$

$$F_{tm} = \int \mathrm{d}^2 r \gamma_{\mathrm{mp}}|\boldsymbol{M}|^2\Big(|\psi_{px}|^2 + |\psi_{py}|^2\Big), \tag{19}$$

$$\begin{aligned} F_{\mathrm{stm}} = \int \mathrm{d}^2 r \Big(& K_{\mathrm{spm}}\big((D_x\psi_{px})^* + (D_y\psi_{py})^*\big)\psi_s \\ & - \big((D_x\psi_s)\psi_{px}^* + (D_y\psi_s)\psi_{py}\big) \\ & + K_{\mathrm{sdpm}}M\big((D_x\psi_{px})^* - (D_y\psi_{py})^*\big)\psi_d \\ & - \big((D_x\psi_d)\psi_{px}^* - (D_y\psi_d)\psi_{py}^*\big) + c.c.\Big). \end{aligned} \tag{20}$$

The last term should incorporate the interaction between the ferromagnetic and superconducting layers and is given as before:

$$\begin{aligned} F_{\mathrm{surf}} = \int_{\mathrm{surf}} \mathrm{d}^2 r \Big(& g_d|\psi_d|^2 + g_s|\psi_s|^2 \\ & + g_{px}|\psi_{px}|^2 + g_{ds}\big(\psi_d\psi_s^* + c.c.\big) - t_m m_0 m\Big), \end{aligned} \tag{21}$$

where g_α ($\alpha = d, s, p_x$) and g_{ds} describe the suppression and the scattering of the SCOP at the interface, respectively. Here, the ferromagnet is treated simply as a source of the magnetization at the interface, and m_0 and t_m denote the value of m at the interface and its tunneling matrix element to the superconducting side, respectively.

All coefficients having indices with a combination of elements from the set s, d, p, m have to be determined from microscopic theories such as the modified Gorkov theory of d-wave superconductors or taken from material properties such as the superconducting coherence length and the magnetic field penetration depth, which depends on the direction. The space of possible coefficients is large. It has been derived from the Hubbard model [22] by Kuboki [13].

We have to solve 11 GL equations following the variational principle of the S–F system. Having the SCOP distribution and the magnetization distribution we can construct the BdGe wavepackets.

It should be emphasized that similar considerations as for a ferromagnet on the top of a superconducting strip can also be applied to an antiferromagnetic strip on the top of a superconductor strip. However, in such a case, the decrease of the SCOP magnitude is expected to be much smaller. In order to confirm the intuitive expectation the solution of extended GL equations derived from the Hubbard model should be obtained, which can be solved, *e.g.*, by the usage of the relaxation method, presented already in this work.

7 Discussion of FIJJ properties In this work the LDOS was computed using the GL + BdGe approach (when the SCOP from GL is used in BdGe) for the case of a two-dimensional system when the non-superconducting and non-magnetic material was placed on the top of an s-wave superconductor, as depicted in Fig. 2 for two different temperatures. Since the conductivity of the given structure is proportional to the LDOS, such an obtained solution can be verified experimentally. Additionally, the hybrid approach using the GL + BdGe formalism significantly speeds up the computation, because we use the thermodynamic approach of the GL formalism, which omits a more detailed and technically involving microscopic picture. However, at the same time such an approach lowers the precision of the computation. Nevertheless, in such an approach we obtain a qualitative structure of eigenenergies present in the FIJJ structure. This gives a hint of the system reaction to the external microwave field as coming from external EM radiation.

For a thick superconducting strip and a thin ferromagnetic layer on the top without an external magnetic field the Josephson effect may be very weak or not observable at all. Yet bringing the whole structure into the external magnetic field will eventually lower the SCOP, especially in the superconductor beneath the ferromagnetic bar, so it will separate one reservoir of the superconducting electrons into two reservoirs.

If we place the given Josephson junction structure in an external magnetic field, it is rather natural to expect a reduction of the superconducting critical current. However, if the FIJJ junction is in quasi-tunneling weak link regime, the analogies of this structure with an S–F–S JJ start to be apparent. In such a case the dependence of the junction critical current on the magnetization of the F strip is described by a damped sinusoidal function. Therefore, the higher magnetization of the F strip does not always reduce the critical current of the FIJJ.

Consider now the superconductors of the second type with ferromagnetic material on the top. In those structures magnetic field vortices can appear in certain situations. The superconductor–ferromagnet interface generates a vortex pinning mechanism depending on the number of crystal defects in materials, direction of magnetization of the ferromagnetic bar and initial configuration of the external magnetic field. In the presence of the electric current flowing via the FIJJ those vortices can move due to the Lorentz force and generate additional dissipation in the system.

Hence, vortices affect both the DC and AC FIJJ current–voltage characteristics. Therefore, the magnetic field induced crossover from flux-flow to Josephson-junction behavior is interesting, as pointed out by Horide [18]. In particular, the presence of vortices should increase the sensitivity of a *d*-wave FIJJ to detect microwave radiation, since the vortex quasi-normal cores absorb EM radiation more effectively than in an *s*-wave superconductor.

The physics of vortices in an *s*-wave superconductor is far more simple than in the case of a *d*-wave superconductor, as presented in Ref. [19]. In the same way, the properties of vortices in FIJJ structures are simpler for an isotropic superconductor than in the case of an anisotropic superconductor. It is important to note that the presence of vortices can induce a Josephson junction in the S–SF–S (superconductor–ferromagnet on top of superconductor–superconductor) system.

8 Summary and outlook The SCOP and magnetization for the MFIJJ were derived from the extended GL equations. They can be used for future determination of the basic transport properties of the FIJJ. The solution of the GL equations for FIJJ structures can be characterized by two regimes of the SCOP distribution named the constriction weak link regime and the quasi-tunneling weak link regime. The weak link constriction regime of the FIJJ is named due to the fact that the SCOP distribution, which has a certain narrowing caused by the presence of the non-superconducting strip, is lowered, but it is not diminishing completely as depicted in Figs. 2 and 3. Therefore, the transmission coefficient should be rather high. On the other hand, the case of a quasi-tunneling weak link Josephson junction is characterized by an almost complete disappearance of the SCOP in the region under the non-superconducting strip as it is in the S–F–S (superconductor–ferromagnet–superconductor) Josephson junction. In such a case the transmission coefficient should be much smaller than in the previous case.

When the magnetization of F (*e.g.*, Fe) is high enough, the superconductor under the F element becomes normal and usually conductive, as it is the case of low-temperature superconductors. However, the given superconductor can also transfer to a normal state, which is insulating as in the case of YBCO material (*d*-wave superconductor). Then the insulating state can exist between two superconducting states, justifying the use of the term: quasi-tunneling weak link.

The transition from the constriction weak link to the quasi-tunneling weak link has been obtained numerically for *s*-wave superconductors by a continuous change of thickness of the superconductor strip or by a continuous change of the magnetization strength of the F bar. The existence of the transition, as depicted in Fig. 3, gives the basis for possible applications of FIJJs and tunable devices built from FIJJs such as FIJJ SQUIDs. The tuning property of the FIJJ should be confirmed experimentally. Similar reasoning applies to the case of usage of a ferroic element instead of a ferromagnetic one. In the limited temperature regime, it is possible to transfer the SCOP and magnetization from GL equations to Usadel propagator equations. Then the approximated current–voltage characteristics, critical superconducting current and critical superconducting temperature can be obtained and related to the system geometry, external magnetic field and magnetization profile of the FIJJ.

Acknowledgements We thank A. Bednorz, W. Bardyszewski, P. Jakubczyk, M. Sznajder, and J. Lawrynowicz for useful comments and remarks.

References

[1] B. Josephson, Phys. Lett. **1**, 251 (1961).
[2] K. K. Likharev, Rev. Mod. Phys. **51**, 101 (1979).
[3] T. W. Clinton and M. Johnson, Appl. Phys. **85**, 1637 (1999).
[4] S. Reymond, P. SanGiorgio, M. R. Beasley, J. Kim, and K. Char, Phys. Rev. B **73**, 054505 (2006).
[5] S. Reymond, P. SanGiorgio, M. R. Beasley, J. Kim, T. Kim, and K. Char, SLAC-PUB-13945 (2008).
[6] A. Maeda, K. Ota, Y. Imai, D. Nakamura, R. Tanaka, H. Kitano, I. Tsukada, M. Hanawa, L. Gomez, K. Hamada, R. Takemura, M. Ohmaki, M. Suzuki, T. Machi, and K. Tanabe, J. Superconduct. Nov. Magn. **23**, 775 (2010).
[7] K. Pomorski and P. Prokopow, Electron. J. Theor. Phys. **7**, 23 (2010).

[8] N. Cassol-Seewald and G. Krein, Braz. J. Phys. **37**(1A), 37–340 (2007).
[9] Z. Ivanov, J. Phys. Colloq. (France) **39**, 6250 (1978).
[10] P. Lipavsky, K. Morawetz, J. Kolacek, and T. J. Yang, Phys. Rev. B **73**, 052505 (2006).
[11] J. Betouras, Z. Dong, T. Venkatesan, and P. Hadley, Appl. Phys. Lett. **69**, 2432 (1996).
[12] J. J. Vicente Álvarez, C. Balseiro, and G. C. Buscaglia, Phys. Rev. B **58**, 11181 (1998).
[13] K. Kuboki and K. Yano, J. Phys. Soc. Jpn. **81**, 064711 (2012).
[14] K. Kuboki and K. Yano, Phys. Rev. B **70**, 214524 (2004).
[15] K. Usadel, Phys. Rev. Lett. **25**, 507 (1970).
[16] G. Eilenberger, Z. Phys. **214**, 195 (1968).
[17] A. Fetter and J. Walecka, Quantum Theory of Many-Particle Systems (McGraw Hill, New York, 1971).
[18] T. Horide, K. Matsumoto, A. Ichinose, M. Mukaida, Y. Yoshida, and S. Horii, Phys. Rev. B **75**, 020504 (2007).
[19] G. Blatter, M. V. Feigel'man, V. B. Geshkenbein, A. I. Larkin, and V. M. Vinokur, Rev. Mod. Phys. **66**, 1125 (1994).
[20] P. G. de Gennes, Superconductivity of Metals and Alloys (Benjamin, New York, 1966).
[21] D. L. Feder and C. Kallin, Phys. Rev. B **55**, 559 (1996).
[22] J. Hubbard, Proc. R. Soc. A **276**, 238 (1963).
[23] A. I. Buzdin, Rev. Mod. Phys. **77**, 935 (2005).

